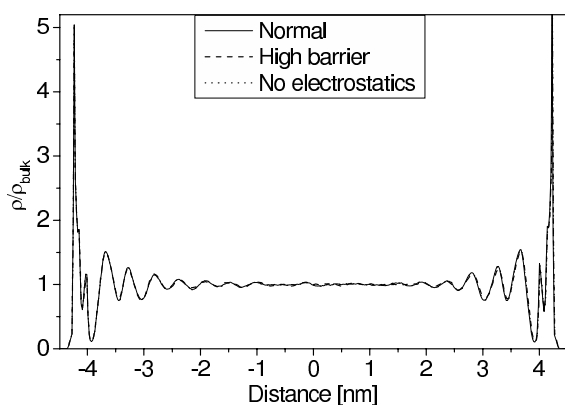
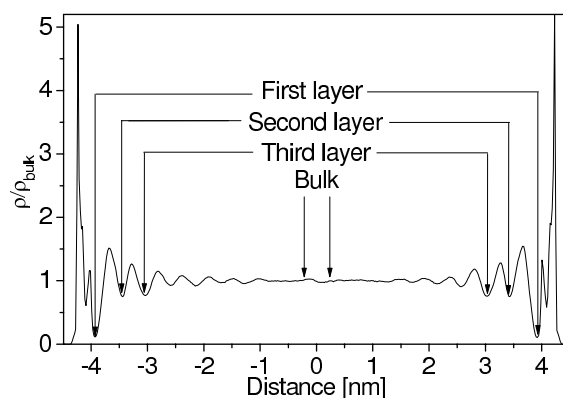


### 6.3.2.1. Density and atoms distribution

The density and atom distribution along the surface normal ( $z$ -axis) was performed for all three systems (Figs. 6.12, 6.13). The density distribution showed oscillations up to about 3 nm from the surface, which are caused by layering of isopropanol molecules.



**Figure 6.12a.**



**Figure 6.12b.**

**Figure 6.12.** The mass density distribution of isopropanol along the surface normal normalized by the bulk density for all three systems (normal, high barrier, and without electrostatic interactions between adsorbate and the surface) (a). The arrows in the figure (b) show, how the layers of the interface for further analysis are defined. The first layer is between the surface and the first minimum after the first peak, the second is between the first and the second minima, etc. There are two instances of each layer on both sides of the slab. The bulk layer is the layer of 0.5 nm thickness located exactly in the center. The boundaries of the *Distance*-axis coincide with positions of the platinum surface (-4.49 nm and 4.49 nm).

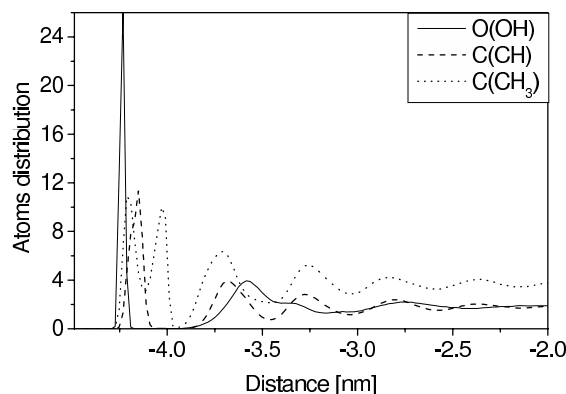


**Figure 6.13.** The distribution of hydroxyl oxygen, methyl and methine carbons along the surface normal. The left boundary of the *Distance*-axis coincides with position of the platinum surface (-4.49 nm). Only one surface of the slab is shown as the profile of distribution is symmetric (see Fig. 6.12).

This is 2 nm further out than for the Pt(111)/water interface<sup>15</sup>. This effect is clearly due to the larger size of isopropanol molecule. Still, there remains a difference between water and isopropanol: water becomes essentially unstructured after the third layer, whereas for isopropanol, small density variations are still visible at the position of layer eight. The distributions are the same for the system with a higher lateral translational barrier (10 kJ/mol instead of 5 kJ/mol) along the bridge site and for the system with no electrostatic interactions. This means that the presence of electrostatics or higher barrier (lower mobility of the adsorbed layers) hardly influences this static property.

The distribution of the oxygen and carbons of isopropanol in the first directly attached layer (-4.2 to -3.9 nm) (Fig. 6.13) shows that mainly two groups are immediately adsorbed onto the surface. These are the hydroxyl oxygens (maximum at  $\sim 0.25$  nm from the surface) and a fraction of the methyl groups ( $\sim 0.27$  nm). Only few molecules are located in such a way that the methine groups have direct contact with the surface. The presence of two almost equal peaks for methyl groups (the second is at  $\sim 0.45$  nm) could suggest that one preferred adsorption geometry of isopropanol is with one methyl group is directly on the surface and the other one pointing upward, hence, creating a hydrophobic methyl “brush” (Fig. 6.14a). The slightly higher intensity peak of the closer to the surface would then suggest that some of the isopropanol molecules still lie with both methyl groups on the surface (Fig. 6.14b). The analysis of the  $\text{CH}_3\text{-CH-CH}_3$  molecular plane orientation (not shown) and orientational analysis (see 6.3.2.2 section) showed that the non-zero distribution of methyl groups between the peaks corresponds to a subgroup of molecules that have the methine groups in contact with the surface. These molecules have their methyl groups located a bit further from the surface (non-zero distribution of methyl groups between two peaks) and the  $\text{CH}_3\text{-CH}_3$  vector is preferably parallel to the surface (Fig. 6.14c). The saturation coverage of the surface was estimated from average number of molecules in the first layer and was found to be 0.256 (42-43 molecules per 168 surface Pt atoms, slightly above 1:4). The other two systems (high barrier and no surface electrostatics) had the same distributions.

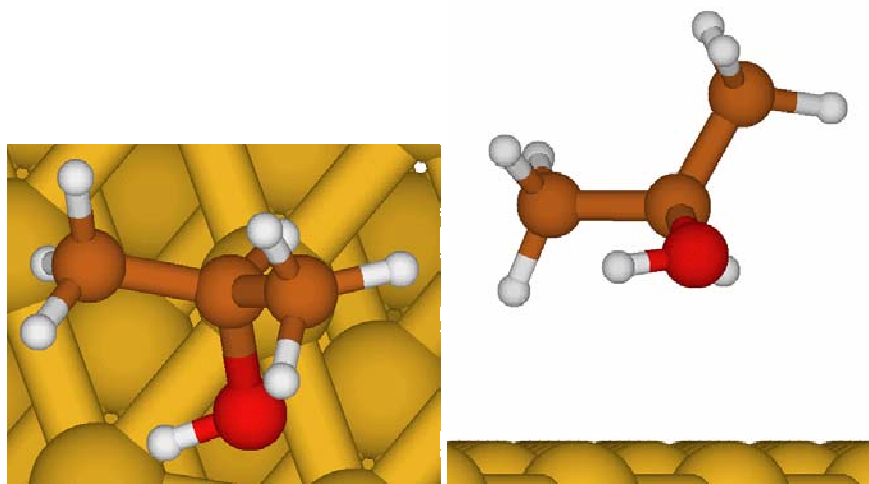


**Figure 6.14a.**

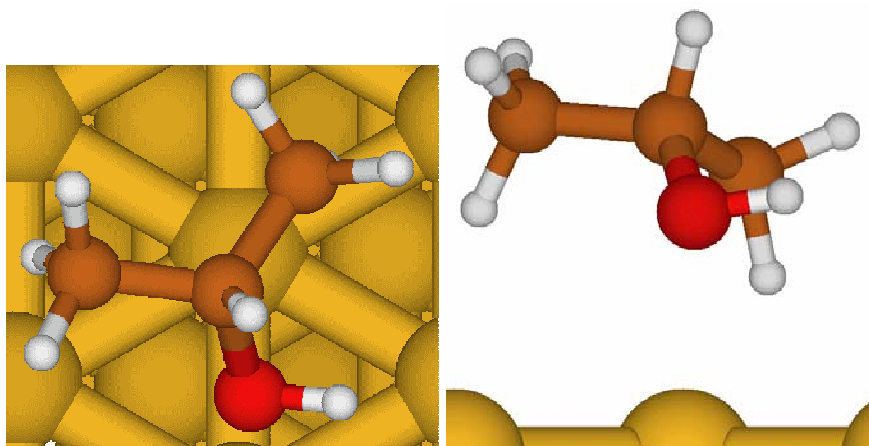


**Figure 6.14b.**

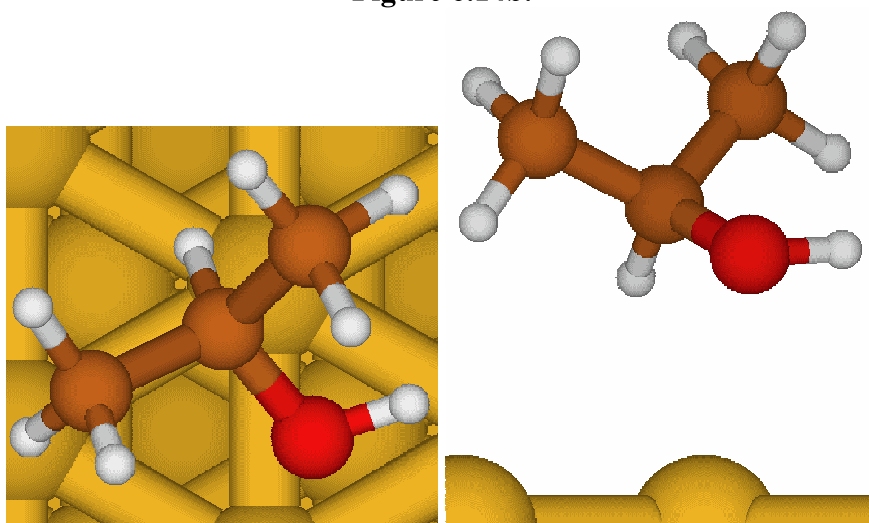


**Figure 6.14c.**

**Figure 6.14.** Three typical orientations of isopropanol molecules in the first layer.

Molecules in the second layer orient preferably with their methyl groups towards the first layer's methyl "brush" and the hydroxyl groups towards the third layer. The third layer's distribution is the inversion of the second layer's (oxygen atoms are closer to the surface than methyl groups), but the pattern is less pronounced. The pattern of alternating atom distributions is also observed in the higher layers, although with decreasing intensity.

Of the adsorbed layer, only the methyl groups are exposed to the next layer of isopropanol. As they are hydrophobic, the second layer is oriented mainly with its methyl groups towards the first one (Fig. 6.13). The peaks of distribution in the higher layers are not pronounced enough to conclude possible orientations. The interaction energy between methyl groups of different isopropanol molecules is less than between hydroxyl groups. Therefore, one could presume that the bulk of isopropanol is attached relatively weakly to the first adsorbed layer and, in general, to the surface. This point is also supported by the much smaller and wider density peaks in the second layer (cf. Fig. 6.12) and also by the two-dimensional in-plane radial distribution functions of Pt-O pairs in the first two layers and in the bulk (Fig. 6.15). The first adsorbed layer has oscillations that suggest that

overall there are sites on the surface, which are more attractive than others. The small magnitude of these oscillations on the other hand suggests implicitly that adsorbed molecules are pretty mobile. Boltzmann inversion of the RDF gives barrier free energies of 0.1-0.3kT. In the second and the bulk layer there are no lateral variations, and the RDF is approximately 1 at all distances. Molecules from the second layer onward have no preferred lateral positions relative to the surface and, very likely, diffuse freely in the  $xy$  plane. The same picture holds for the system with no surface electrostatics. The oscillations of the first layer RDF become, however, much more pronounced as the translation barrier of a molecule adsorbed directly on the surface is increased (free energy  $\sim 2.3kT$ , Fig. 6.16).

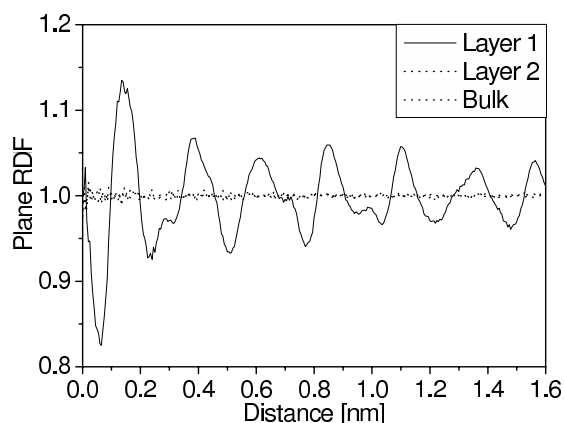


**Figure 6.15a.**

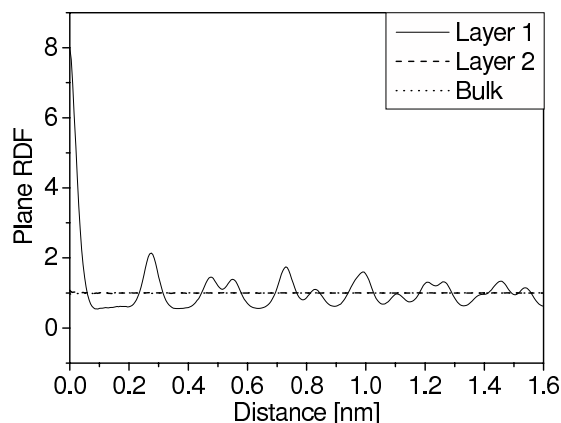


**Figure 6.15b.**

**Figure 6.15.** In-plane radial distribution functions of Pt-O in first, second, and bulk layers for the normal system (a) and the system with high translational barrier (b).

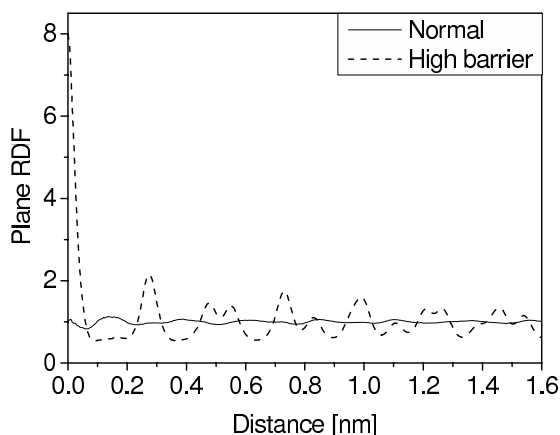


**Figure 6.16.** Comparison of in-plane radial distribution functions Pt-O in the first adsorbed layer of the normal system and the system with high barrier.

The RDF in the second and onward layers showed no differences between all three systems (not shown). Comparing the first adsorbed layers of two systems (normal and high barrier) to each other (Fig. 6.17) revealed that the oscillations in the Pt-O in-plane

RDF for the normal system have no strong correlation with the topology of the surface. However, in the case for the high barrier system it is clear that the positions of peaks correspond to the positions of platinum atoms. This suggests that in the high barrier system compared to the normal system the  $xy$  structuring is more stable relatively to the surface.

The comparison of O-O in-plane RDFs to Pt-O RDFs of the normal and high barrier systems showed that, for the high barrier systems, the O-O distribution in the first layer tends to correlate stronger with the Pt-O RDF than in the normal system, where the translation barrier is lower (Fig. 6.17). The relative structuring at longer distances (1.2-1.6 nm) is more pronounced for the high barrier system than for the normal system and the system without surface electrostatics (the latter two have almost the same in-plane RDFs).

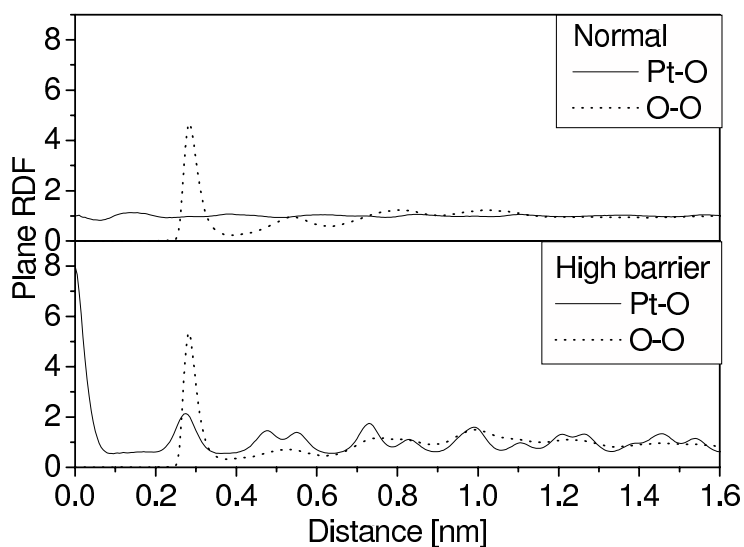


**Figure 6.17.** In-plane radial distribution functions of Pt-O and O-O of isopropanol in the first adsorbed layer for the normal and the high barrier systems.

The analysis of the O-O in-plane RDF within different layers and in the bulk (Fig. 6.18) shows that the in-plane structure vanishes at longer distances ( $> 1$  nm) with the distance of a layer to the surface and becomes more bulk-like. Beyond 1.2 nm, there is no structuring in the second and the third layers. The in-plane RDFs of other groups ( $\text{CH}_3\text{-CH}_3$  and  $\text{CH-CH}$ ) were found to be almost identical for all systems and all layers (not shown).

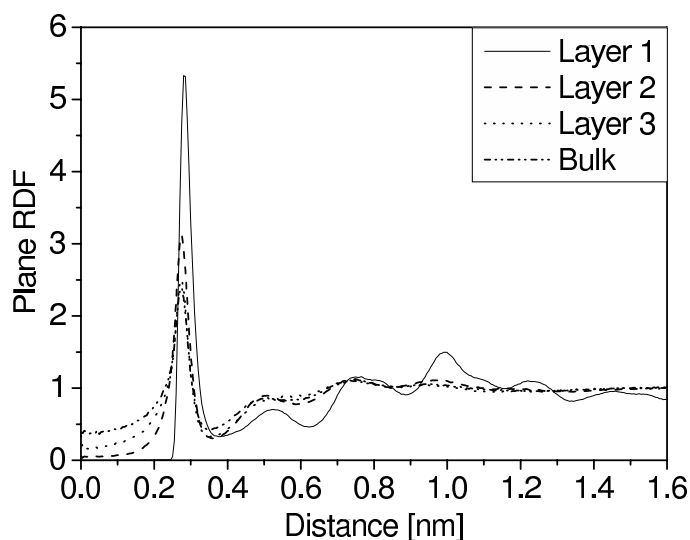


**Figure 6.18.** In-plane radial distribution functions of O-O atoms for the high barrier system in different layers and the bulk.

### 6.3.2.2. Orientation

To study the orientational structure, the order parameter  $S^2 = \frac{1}{2} \langle 3 \cos^2 \theta - 1 \rangle$  as a function of the distance to the surface was studied for different vectors: O-H, O-C(CH), C(CH<sub>3</sub>)-C(CH<sub>3</sub>). For O-H and O-C vectors, the oxygen atom was used to calculate the distance to the surface. For the C-C vector, the center of mass of the methyl groups was used as the reference point.  $\theta$  is the angle between the vector being analyzed and the surface normal.  $S^2 < 0$  signifies a preferential orientation in the surface plane,  $S^2 > 0$  an orientation perpendicular to the surface, and  $S^2 = 0$  a random orientation. Immediately at the interface, the O-H vector is almost always parallel to the surface (Fig. 6.19a), as each hydroxyl group on the surface forms a hydrogen bond with one of the neighbouring adsorbed hydroxyl groups (cf. Fig. 6.18). In the second layer the preferred orientation of O-H vector is also parallel to the surface but with much less degree than in the first, whereas in the third layer it is perpendicular to it. In the higher layers there no orientation is favoured.

The O-C(CH) vector that in the first adsorbed layer prefers to keep parallel to the surface, although with notably less degree of order than in the case of the hydroxyl group (Fig. 6.19b). This constraint is due to the methyl and methine groups of the alcohol as they prevent O-C vector sterically from becoming completely flat. The second layer shows a diverse behaviour: O-C bonds closer to the surface are oriented mainly parallel to the surface, whereas O-C vectors further away are preferentially perpendicular. Recall that the O-H vectors in the entire second layer are mainly parallel to the surface. The detailed investigation of atom and order parameter distributions revealed that the

explanation of such behaviour lies in the atom distribution (Fig. 6.13). The sublayer with O-C bonds parallel to the surface corresponds to only few isopropanol molecules, whose oxygen atoms are closer to the surface. The methyl groups of most of the molecules are pulled towards the methyl “brush” of the first layer, whereas the hydroxyl groups are attracted to the hydroxyl groups in the third layer. Therefore, the O-C bonds of the molecules in the second layer are “stretched” along the surface normal by the methyl and hydroxyl groups. The third layer has exactly the inverted picture (the peak showing the O-C bond orientation perpendicular to the surface is common for the second and the third layers). As in the case of the atom distribution, this inversion pattern repeats itself, with reducing intensity, up to the fifth layer ( $\sim 2.15$  nm) according to the density peaks (cf. Fig. 6.12). Further layers show no preferred orientation of O-C(CH) bonds.

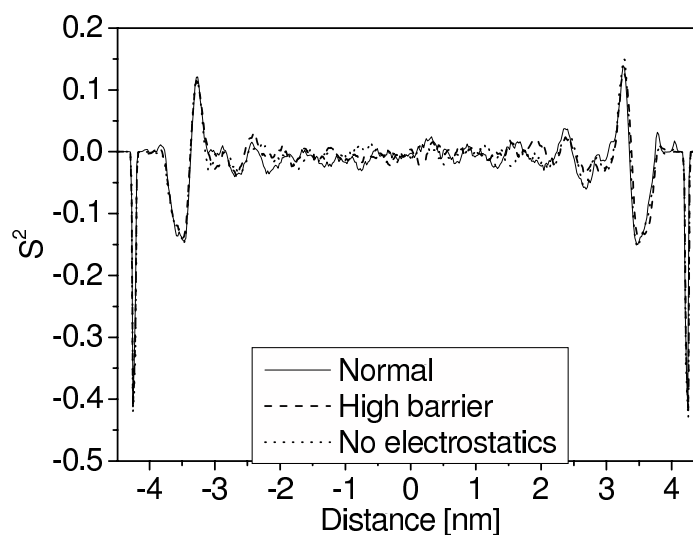


**Figure 6.19a.**

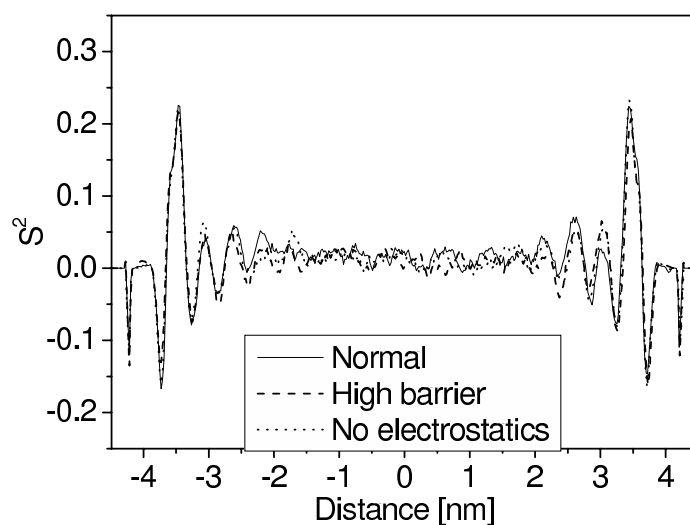


**Figure 6.19b.**

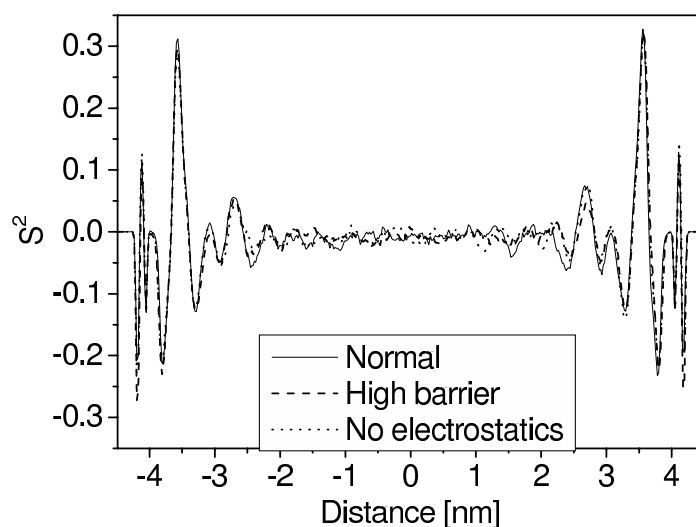


**Figure 6.19c.**

**Figure 6.19.** The order parameter  $S^2$  as a function of distance of molecular vectors O-H (a), O-C(CH<sub>3</sub>) (b), and C(CH<sub>3</sub>)-C(CH<sub>3</sub>) (c) for the normal system, the system with high barrier, and with no electrostatic interactions between the surface and the adsorbate. For the O-H and O-C vectors, the position of the oxygen atom was used to calculate the distance. For C-C vector, the center of mass of methyl groups was used. The boundaries of *Distance*-axis coincide with positions of the platinum surface (-4.49 nm and 4.49 nm).

The orientation of the C(CH<sub>3</sub>)-C(CH<sub>3</sub>) vector (Fig. 6.19c) and the C(CH<sub>3</sub>)-C(CH<sub>3</sub>)-C(CH<sub>3</sub>) plane (not shown) in the first layer supports the assumption given in the previous section: the molecules have one methyl on the surface and one of them points away from it. There are also few molecules with both methyl groups on the surface. Other molecules touch the surface with the methine group and, hence, have their methyl groups further from the surface and also the C-C vector preferably parallel to it (see Figs. 6.13, 6.14). The second layer has two sublayers: in the one closer to the surface, the C-C vector is parallel to the surface and in the following it is perpendicular. Again, as in the case of O-C bond this pattern is determined by the atom distribution (Fig. 6.13). Most of the molecules in the layer have their methyl group attached onto the methyl “brush” of the first layer. This obviously results in a parallel orientation of the CH<sub>3</sub>-CH<sub>3</sub> vector. Only few molecules at the connection of the second and the third layer correspond to the orientation perpendicular to the surface. Once more, in the third layer this picture gets inverted and this inversion pattern extends up to the fifth layer, but with reducing intensity. At further distances there is almost no preferred orientation. All three investigated systems showed the same behaviour.

It is also clear from Fig. 6.19 that electrostatic interactions between isopropanol and the surface have no visible effect on the orientation of the O-H vector along the *z* axis, although both atoms – oxygen and hydrogen – have notable partial charges (-0.7e and +0.4e). Therefore one can conclude that, if the adsorbate molecules have inhomogeneous distribution of charges and even weak chemical interactions with the metal surface, the geometry of the first layer is driven by this chemical adsorption and



lateral interactions. The geometry of the following layers is determined by the first adsorbed layer. However, the electrostatic response of the metal might play a more prominent role in systems where the chemical interactions are weaker or where charged species are present.

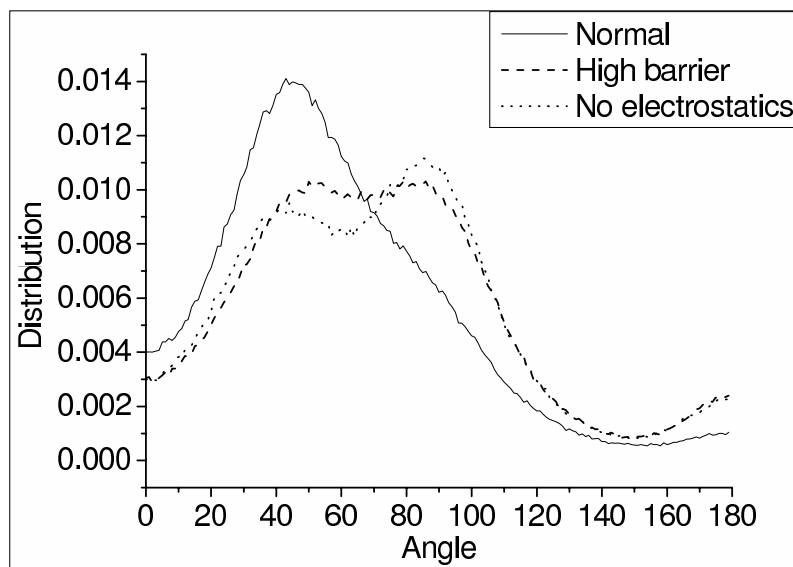


**Figure 6.20.** Angle distribution between vectors defined by O-H bonds of isopropanol molecules in the first adsorbed layer, whose oxygen atoms are at the distance up to the first minimum in the O-O plane radial distribution function (Fig. 6.18) ( $< 0.38$  nm).

The distribution of angles between O-H bonds of isopropanol molecules was studied (OH-OH angle) for all three systems (Fig. 6.20) in all layers. Only the molecules, whose oxygen atoms are located within the shell up to first minimum in the O-O plane RDF (Fig. 6.18) (i.e.  $< 0.38$  nm), were considered. These molecules can potentially form hydrogen bonds. There are obviously two maxima, one at 40-50°, the other one around 90°, whose relative population and precise position depend on the model. In the first adsorbed layer (Fig. 6.20), the angle distribution depends on the translational barrier of an adsorbed molecule as well as on the electrostatic response of the metal. The electrostatic interactions of adsorbate molecules with the surface introduce additional forces that can change the orientation of O-H bonds relative to each other and, therefore, the average OH-OH angle distribution. The influence of the higher translational barrier may have its origin in the fact that molecules are more confined to the atop sites. Thus, the OH-OH angle is influenced more by the surface structure. The angle distribution in the second, third, and bulk layer are the same for all systems.

### 6.3.2.3. Mobility and exchange dynamics

The center-of-mass mean square displacement in the  $x$ - $y$  plane (MSD) of isopropanol molecules was calculated in order to address the mobility of those molecules in different layers and different systems (Fig. 6.21). The MSDs were calculated over all time origins of all periods when a center of mass of a molecule stayed within the given slab. The displacement of the molecules in the first layer in the normal system is expectedly larger than that one of the system with high barrier (Fig. 6.21a). The system with the electrostatic interactions between adsorbate and the surface switched off also shows slower diffusion of molecules at the interface. At times up to about 100ps, however, this system has molecules slightly faster than in the normal system. This result is expected, as the contribution of the electrostatic interaction to the potential barrier is small but still present in the normal system (the atop site is more attractive electrostatically than the hollow site<sup>23</sup>). The slower diffusion at longer times might be due to the lack of statistics available for longer times. Additionally, there are only few molecules (42-43) adsorbed directly at each interface, which also reduces the sampling space. In the higher layers and the bulk there is no difference in the mobility due to the different models (not shown). The MSDs are very similar, and different rankings are due to statistics.

The comparison of the molecular mobility in different layers of the interface in the normal system shows that the molecules adsorbed onto the surface have the lowest mobility of all (Fig. 6.22). The mobility of molecules increases with the distance to the surface. The lateral diffusion in the surface layer is, thus, about 2.5 times slower than in the bulk. For the high barrier system, the diffusion coefficient in the first layer is about 2 times lower, whereas in the bulk it is unchanged.

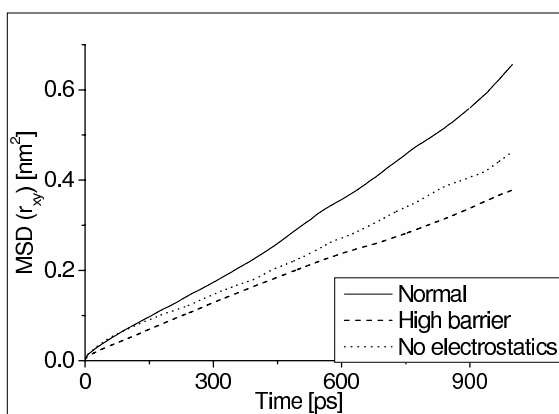


**Figure 6.21.** The mean in-plane square displacement of center of mass of isopropanol molecules in the first immediately adsorbed layer for the normal system, the system with high translational barrier, and the system with no electrostatic interaction between isopropanol and the platinum surface.

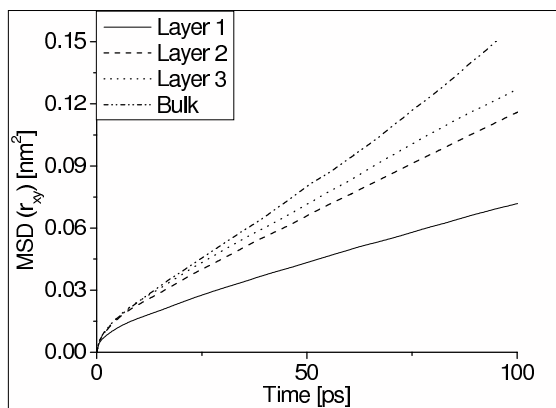


**Figure 6.22.** The in-plane mean square displacement of center of mass of isopropanol molecules in the first immediately adsorbed, second, third, and the bulk layers for the normal system.

The distribution of the residence time in different layers was also calculated for all systems. The residence time was calculated as the difference between two time points: when the center of mass comes into a certain slab and when it leaves it. For the first adsorbed layer, the simulations are still too short and the graph of the distribution is rather meaningless (not shown).

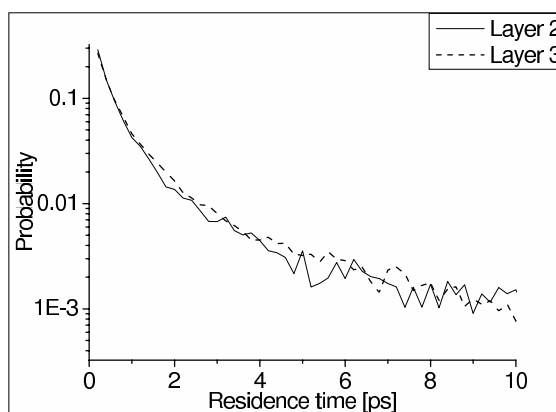


**Figure 6.23.** The semi-log plot of the residence time distribution for the center of mass of isopropanol molecules in the second and third layers for the normal system. For the other systems the distributions are almost the same.

Most of the molecules never leave this layer during the simulations ( $\sim 3$  ns). Only few events ( $\sim 10$ ) of desorption after residence times of 20 ps and longer were registered. The three systems showed no qualitative difference in this respect. The residence time distribution in the higher layers appears to be the same for all systems (Fig. 6.23). This suggests that the interactions with the surface hardly influence the exchange dynamics of molecules in the second and the third layers of the interface.

## 6.4. Summary and conclusions

A model is devised and parameterized to study the platinum(111)/isopropanol interface by means of molecular dynamics (MD) simulations. In addition to the classical MD interaction potentials (Lennard-Jones and interaction of point charges) two more types of interactions were included in the model. The first is the electrostatic interaction of isopropanol molecules with the metal surface. The second is a short range attraction potential to mimic the partial chemical bond between the hydroxyl oxygen and the platinum atoms. Additionally, the possible influence of the chemical adsorbate-surface interactions and of the electrostatic response of the metal surface was investigated.

The adsorption energy as a function of coverage decreases up to the 32 molecules ( $\sim 3/4$  of the saturation level). The adsorption energy for the multilayer was found to reduce gradually with the increase of the coverage, which corresponds to the finding by Panja *et al.* from their TPD experiment<sup>25</sup>.

Analysis of the density as a function of distance to the surface showed that there is a strong packing of molecules at the surface followed by a depletion layer with very low density. These two layers are then followed by an oscillating density profile up to 3 nm from the surface. The distribution of individual atom types as a function of distance revealed that isopropanol molecules adsorb on the surface with their hydroxyl oxygen and mainly one methyl group per molecule. The other methyl group is sticking up, thus, creating a hydrophobic methyl “brush” above the adsorbed hydroxyl groups. In the following second layer molecules prefer to orient their methyl groups towards the first layer. Since methyl-methyl interactions are notably weaker than hydrogen bonds between hydroxyl groups of different molecules, one can assume that the second and the following layers are not strongly attached to the adsorbed layer. The same is also suggested by the much smaller and wider density peak in the second adsorbed layer, which means that the platinum surface with one layer of adsorbed isopropanol is much less attractive. Moreover, the planar radial distribution functions (RDF) of platinum and oxygen atoms in the first layer of the interface showed oscillations that point out the presence of preferred sticky atop sites on the surface. The RDFs of the following layers showed no preferred positions in any systems. This effect implicitly shows a higher and more uniform mobility of molecules in the second and higher layers. It might be one more proof of weak interlayer adhesion.

The orientational structure was studied by calculation of the order parameter of O-H and O-C(CH<sub>3</sub>) vectors as the function of distance to the surface. Surprisingly, it was found that the electrostatic response of the metal surface to the electrical field created by the adsorbate molecules hardly influences this property. In contrast, the relative orientation of neighbouring hydroxyl groups that can form hydrogen bonds in the first layer is notably influenced by both the electrostatic response of the metal surface and the translational barrier.

## *6.5. Acknowledgements*

The authors are thankful to the Hochschulrechenzentrum der Technische Universität Darmstadt for the granted time on the IBM Regatta p575 machines (HHLR) located at the TU Darmstadt, Darmstadt, Germany.

## 6.6. References

- (1) Shipway, A. N.; Katz, E.; Willner, I. *ChemPhysChem* **2000**, *1*, 18.
- (2) Boennemann, H.; Richards, R. M. *Eur. J. Inorg. Chem.* **2001**, *2001*, 2455.
- (3) Liu, J. C.; Anand, M.; Roberts, C. B. *Langmuir* **2006**, *22*, 3964.
- (4) Toshima, N.; Shiraishi, Y.; Teranishi, T.; Miyake, M.; Tominaga, T.; Watanabe, H.; Brijoux, W.; Bonnemann, H.; Schmid, G. *Appl. Organomet. Chem.* **2001**, *15*, 178.
- (5) Porta, F.; Prati, L.; Rossi, M.; Scari, G. *J. Catal.* **2002**, *211*, 464.
- (6) Delle Site, L.; Alavi, A.; Abrams, C. F. *Phys. Rev. B* **2003**, *67*.
- (7) Delle Site, L.; Sebastiani, D. *Phys. Rev. B* **2004**, *70*.
- (8) Jacob, T.; Goddard, W. A. *J. Am. Chem.* **2004**, *126*, 9360.
- (9) Jacob, T.; Muller, R. P.; Goddard, W. A. *J. Phys. Chem. B* **2003**, *107*, 9465.
- (10) Meng, S.; Wang, E. G.; Gao, S. W. *J. Chem. Phys.* **2003**, *119*, 7617.
- (11) Meng, S.; Wang, E. G.; Gao, S. W. *Phys. Rev. B* **2004**, *69*.
- (12) Mittendorfer, F.; Hafner, J. *Surf. Sci.* **2001**, *472*, 133.
- (13) Lee, S. H.; Kim, H. S. *Bull. Korean Chem. Soc.* **1996**, *17*, 700.
- (14) Kohlmeyer, A.; Witschel, W.; Spohr, E. *Chem. Phys.* **1996**, *213*, 211.
- (15) Raghavan, K.; Foster, K.; Motakabbir, K.; Berkowitz, M. *J. Chem. Phys.* **1991**, *94*, 2110.
- (16) Zhu, S. B.; Philpott, M. R. *J. Chem. Phys.* **1994**, *100*, 6961.
- (17) Jhon, Y. I.; Kim, H. G.; Jhon, M. S. *J. Colloid Interface Sci.* **2003**, *260*, 9.
- (18) Abrams, C. F.; Delle Site, L.; Kremer, K. *Phys. Rev. E* **2003**, *67*.
- (19) Schravendijk, P.; van der Vegt, N.; Delle Site, L.; Kremer, K. *ChemPhysChem* **2005**, *6*, 1866.
- (20) Witek, H.; Buch, V. *J. Chem. Phys.* **1999**, *110*, 3168.
- (21) Allen, M. P.; Tildesley, D. J. *Computer Simulation of Liquids*; Oxford University Press: Oxford, 1987.
- (22) Marmier, A.; Hoang, P. N. M.; Picaud, S.; Girardet, C.; Lynden-Bell, R. M. *J. Chem. Phys.* **1998**, *109*, 3245.
- (23) Finnis, M. W. *Surf. Sci.* **1991**, *241*, 61.
- (24) Finnis, M. W.; Kaschner, R.; Kruse, C.; Furthmuller, J.; Scheffler, M. *J. Phys.-Condes. Matter* **1995**, *7*, 2001.
- (25) Panja, C.; Saliba, N.; Koel, B. E. *Surf. Sci.* **1998**, *395*, 248.
- (26) Sexton, B. A.; Rendulic, K. D.; Hughes, A. E. *Surf. Sci.* **1982**, *121*, 181.
- (27) Plsek, J.; Hruby, P.; Nikiforov, K.; Knor, Z. *Appl. Surf. Sci.* **2005**, *252*, 1553.
- (28) Izvekov, S.; Mazzolo, A.; VanOpdorp, K.; Voth, G. A. *J. Chem. Phys.* **2001**, *114*, 3248.
- (29) Izvekov, S.; Voth, G. A. *J. Chem. Phys.* **2001**, *115*, 7196.
- (30) Kiejna, A. *Prog. Surf. Sci.* **1999**, *61*, 85.
- (31) Price, D. L. *J. Chem. Phys.* **2000**, *112*, 2973.
- (32) Kovalenko, A.; Hirata, F. *J. Chem. Phys.* **1999**, *110*, 10095.
- (33) Shelley, J. C.; Patey, G. N.; Berard, D. R.; Torrie, G. M. *J. Chem. Phys.* **1997**, *107*, 2122.

- (34) Velde, G. T.; Bickelhaupt, F. M.; Baerends, E. J.; Guerra, C. F.; Van Gisbergen, S. J. A.; Snijders, J. G.; Ziegler, T. *J. Comput. Chem.* **2001**, *22*, 931.
- (35) Vosko, S. H.; Wilk, L.; Nusair, M. *Can. J. Phys.* **1980**, *58*, 1200.
- (36) Becke, A. D. *Phys. Rev. A* **1988**, *38*, 3098.
- (37) Perdew, J. P. *Phys. Rev. B* **1986**, *33*, 8822.
- (38) van Lenthe, E.; Baerends, E. J.; Snijders, J. G. *J. Chem. Phys.* **1993**, *99*, 4597.
- (39) van Lenthe, E.; Baerends, E. J.; Snijders, J. G. *J. Chem. Phys.* **1994**, *101*, 9783.
- (40) van Lenthe, E.; Ehlers, A.; Baerends, E. J. *J. Chem. Phys.* **1999**, *110*, 8943.
- (41) van Lenthe, E.; Snijders, J. G.; Baerends, E. J. *J. Chem. Phys.* **1996**, *105*, 6505.
- (42) van Lenthe, E.; van Leeuwen, R.; Baerends, E. J.; Snijders, J. G. *Int. J. Quantum Chem.* **1996**, *57*, 281.
- (43) Bauschlicher, C. W. *J. Chem. Phys.* **1985**, *83*, 3129.
- (44) Muller, J. E.; Harris, J. *Phys. Rev. Lett.* **1984**, *53*, 2493.
- (45) Kua, J.; Goddard, W. A. *J. Phys. Chem. B* **1998**, *102*, 9481.
- (46) Curulla, D.; Clotet, A.; Ricart, J. M.; Illas, F. *J. Phys. Chem. B* **1999**, *103*, 5246.
- (47) Garcia-Hernandez, M.; Curulla, D.; Clotet, A.; Illas, F. *J. Chem. Phys.* **2000**, *113*, 364.
- (48) Jing, Z.; Whitten, J. L. *Surf. Sci.* **1991**, *250*, 147.
- (49) Wyckoff, R. W. G. *Crystal Structures*, 2nd ed.; Interscience: New York, 1963.
- (50) McAdon, M. H.; Goddard, W. A. *Phys. Rev. Lett.* **1985**, *55*, 2563.
- (51) Kua, J.; Goddard, W. A. *J. Phys. Chem. B* **1998**, *102*, 9492.
- (52) Berendsen, H. J. C.; Grigera, J. R.; Straatsma, T. P. *J. Phys. Chem.* **1987**, *91*, 6269.
- (53) Glebov, A.; Graham, A. P.; Menzel, A.; Toennies, J. P. *J. Chem. Phys.* **1997**, *106*, 9382.
- (54) Müller-Plathe, F. *Mol. Simul.* **1996**, *18*, 133.
- (55) Müller-Plathe, F.; van Gunsteren, W. F. *Polymer* **1997**, *38*, 2259.
- (56) Müller-Plathe, F.; Brown, D. *Comput. Phys. Commun.* **1991**, *64*, 7.
- (57) McCammon, J. A.; Harvey, S. C. *Dynamics of Proteins and Nucleic Acids*; Cambridge Univ. Press: Cambridge, 1987.
- (58) Ryckaert, J. P.; Ciccotti, G.; Berendsen, H. J. C. *J. Comput. Phys.* **1977**, *23*, 327.
- (59) Müller-Plathe, F. *Comput. Phys. Commun.* **1990**, *61*, 285.
- (60) Müller-Plathe, F. *Comput. Phys. Commun.* **1993**, *78*, 77.
- (61) Tarmyshov, K. B.; Müller-Plathe, F. *J. Chem Inf. Model.* **2005**, *45*, 1943.
- (62) Berendsen, H. J. C.; Postma, J. P. M.; van Gunsteren, W. F.; Dinola, A.; Haak, J. R. *J. Chem. Phys.* **1984**, *81*, 3684.
- (63) Frenkel, D.; Smit, B. *Understanding Molecular Simulation: From Algorithms to Applications*, 2nd ed.; Academic Press: San Diego, 2002.





## 7. Outlook

### *7.1. Parallel molecular dynamics simulations*

One can split development of molecular dynamics simulations into three main streams: development of new and improvement of old simulation methods (i.e. coarse graining<sup>1-3</sup>, multiscale Monte Carlo<sup>4</sup>), development of new and alternative force-fields (i.e. polarizable water molecules<sup>5</sup>, ethanol<sup>6</sup> or poly-vinyl-alcohol<sup>7</sup>), and development of faster and more efficient MD simulation codes. The latter is mainly concentrated on the development of parallel codes that permit to increase system size and to decrease simulation time spans. The development in chemistry requires now the investigation of larger systems (membranes, surfaces, polymer/solid surface interfaces) and larger molecules (longer [more realistic] polymers, proteins, DNA) for longer times. The need for longer times arises from the natural time scales in these systems: melts of long polymer relax only within microseconds, a long protein folding/unfolding process might take up to minutes of time.

Even the increasing capacity of processors cannot keep pace with the growing demands of science. Therefore, one tries and uses more sophisticated methods and tools to access larger systems and longer time scales. Parallelization of molecular simulation codes is rapidly progressing. This has been made possible by the development of special computer architectures (“many processors” – shared memory) and high-speed networks (“many networked computers” – distributed memory).

Chapter 4 describes one possible parallelization strategy for a multi-processor platform. It was shown that the conversion of a sequential code into such parallel one is relatively easy. Yet, this type of parallel simulation is usually limited to 10-20 processors, which means that it reaches only for intermediate speed-up. One can speed-up calculations by up to a factor of 8 (for the test platform – IBM Regatta p690+) and/or increase the size of the simulated system up to, perhaps, hundreds of thousand of atoms.

The usage of distributed memory approach seems to be more promising in terms of the system size simulated (millions of particles) and the number of processors which can be used efficiently (hundreds or thousands). However, for systems where the long range interactions present (highly charged systems) the usage of this approach may be precluded as atoms will be interacting still at too long distances. Consequently, this would cause intensive communication between computers and, as a result, poor efficiency.

In conclusion, one can say that a parallel simulation code should be chosen for each selected molecular system basing on its physics and chemistry to achieve the highest efficiency. Simulation codes parallelized through the shared memory approach will very likely be convenient for usage by academic and industrial groups to solve small and medium complexity problems. Some of these problems can be the preliminary testing of a theory or a model, simulations of small and medium sized molecular melts and solutions, relaxation of small systems followed by the simulations of similar large ones

obtained via the replication of the small system. Distributed memory simulation codes, as one can expect, will fill the niche of simulating very sophisticated systems, where the large size of the system and large number of particles are inescapable.

## 7.2. Cucurbit[n]urils – a novel receptor in molecular recognition

Although the family of cucurbit[n]urils (CBs) was discovered over a century ago, intensive studies started only during the last 25 years. CB[6] dissolves poorly in water, and slightly better – in aqueous salt solutions. In fact, CB[6] is soluble only in highly acidic solutions. Therefore, some work is directed at developing CB[6] and CB[5] derivatives which are soluble well in water or organic solvents<sup>8,9</sup>. CB[7] happens to be acceptably soluble in water and, therefore, is used more intensively in experimental work<sup>10-15</sup>. It has been discovered that CBs are capable of capturing guest molecules and this process can be controlled by the pH which, in turn, controls competition between H<sup>+</sup> and guests for the CB[n] molecule. CB[n]-based molecular switches were also reported: the complexation geometry is controlled by the pH, which results in different protonation states of a guest molecule. There are studies devoted to the production of CB[n] derivatives (i.e. Me<sub>10</sub>CB[5]) and their change in affinity towards certain guests comparing to original CB[n] molecule. (A good review of recent research of CB[n] family and their applications was prepared by Lagona *et al.*<sup>16</sup>)

The pH-controlled capture and release of guests by CBs can also happen with the help of metal cations. Cations are able to seal the cyclic portals of CB[6] and capture the guest inside the cavity, whereas protonation of CBs (low pH) destroys the metal cation “lid” and releases the guest molecule. Molecular simulations are able to attain deeper understanding in what is actually going on at the portals and in the cavity of CB[6] and prove, disapprove, or correct the current experimental model for the process. Chapter 5 presents the results of research on binding of various metal cations to CBs portals and their influence on static and dynamic properties of the molecule was studied by means of molecular dynamics simulations.

Today, the research is carried out to study of changes in the photophysical and photochemical behaviour<sup>12-15</sup>, and changes in the acidity constant of other molecules upon complexation with CBs. For instance, such study of the dye neutral-red (protonated and unprotonated) revealed that the  $pK_a$  value is shifted by 2 units (becomes stronger base) upon complexation<sup>15</sup>. The fluorescence and quantum yields increase substantially when complexed with CB[7]<sup>15</sup>. In these studies, molecular simulations can help us understand the complexation mechanism in more details (precise reaction pathway) and can compare the process for protonated and unprotonated guest. It is also quite desirable to be able to predict the  $pK_a$  shift in order to define the required environment (pH) where the experimental studies should be carried out.

The force-field for CB[6] used in this work was derived from the force-field of tetramethylurea (TMU). One can rely on parameters of carbonyl oxygens, to which metal cations bind, as the neighbouring atoms are the same as in TMU. However, the

parameters of atoms that line the cavity of CB[6] need to be refined if one wants to simulate the capture process. Atom connectivity difference between CB[6] and TMU definitely influences the electron density distribution and, thus, the parameters of those atoms. More adequate force-field can be derived from other molecules with similar atom connectivities and structure, orientation of encapsulated guest in the cavity, and maybe energies of encapsulation obtained from quantum calculations.

### 7.3. *Metal-polymer interfaces*

The investigation of the metal-polymer interfaces with molecular simulations is a quite challenging area and there remains a lot of work to be done. The current research in this field is still not well established despite importance of such interfaces and their properties in industry and our every-day life. This is due to the very complicated electronic structure of metal surfaces and, in particular, of transition metals.

The models, which are available for molecular simulations of metal surface at the interface with other compounds, have been obtained each for a particular system and cannot be easily transferred to something else. An attempt to devise a model and a defined parameterization procedure was made in this work, the results for Pt-isopropanol being reported in Chapter 6. It has been found that the electrostatic response of the metal surface has no visible influence on most properties. The only notable dependence on this type of interactions was found in the formation of hydrogen bonds between isopropanol molecules in the intermediate layer adsorbed onto metal surface. Further layers showed no sensitivity to these interactions.

Such finding can be marked as “unfortunate” for the scientists who deal with the simulations where catalyzed reactions take place (e.g. fuel cells), as the relative orientation of molecules at the metal surface can influence reaction rates. The model for the electrostatic response of metal (DCM) demands significant computational resources. Since in adhesion this relative orientation plays no important role, the DCM can be removed from the simulations. The only task to take care of is chemical adsorption, which appears to happen quite often when transitional metals are involved. However, one has to introduce separate adsorption potentials for each specific system, as adsorption is strongly dependent on the electronic structure of the adsorbate.

It has been also found that the first layer of isopropanol molecules adsorbes mainly via their oxygens. This causes a hydrophobic methyl brush which, in turn, forces the second layer to orient with its methyl groups towards the first layer. The methyl-methyl interactions are quite weak and, as a result of that, the adhesion of the bulk on to the first layer is weak as well. This hypothesis can be clarified using shear simulations and finding the position in the interface where slip takes place.

In case of polymers one can expect that chains will not be adsorbed completely on the surface, but penetrate different layers of the interface. This will most certainly improve interconnectivity between the adsorbed layer and the bulk. An interesting point to investigate for short oligomers or polymers will be the influence of tacticity on the strength of the adhesion to the surface and inter-layer connectivity. The idea is that while

some hydroxyl groups adsorb on the surface, the others (due to relative sterical arrangement caused by tacticity) might be pointing towards the second layer. This may also change properties of the interface. It is also of interest what geometry of oligomer chains will be when each monomer of it can adsorb onto the surface, unlike the study of Abrams *et al.* where chains' can ends can adsorb onto the surface<sup>17</sup>.

## 7.4. References

- (1) Milano, G.; Müller-Plathe, F. *J. Phys. Chem. B* 2005, *109*, 18609.
- (2) Milano, G.; Goudeau, S.; Müller-Plathe, F. *J. Polym. Sci. Pt. B-Polym. Phys.* 2005, *43*, 871.
- (3) Muller-Plathe, F. *ChemPhysChem* 2002, *3*, 754.
- (4) Maggs, A. C. *Phys. Rev. Lett.* 2006, *97*.
- (5) Yu, H. B.; van Gunsteren, W. F. *J. Chem. Phys.* 2004, *121*, 9549.
- (6) Müller-Plathe, F. *Mol. Simul.* 1996, *18*, 133.
- (7) Müller-Plathe, F.; van Gunsteren, W. F. *Polymer* 1997, *38*, 2259.
- (8) Lee, J. W.; Samal, S.; Selvapalam, N.; Kim, H. J.; Kim, K. *Accounts Chem. Res.* 2003, *36*, 621.
- (9) Zhao, J. Z.; Kim, H. J.; Oh, J.; Kim, S. Y.; Lee, J. W.; Sakamoto, S.; Yamaguchi, K.; Kim, K. *Angew. Chem. Int. Edit.* 2001, *40*, 4233.
- (10) Sobransingh, D.; Kaifer, A. E. *Chem. Commun.* 2005, 5071.
- (11) Moon, K.; Kaifer, A. E. *Org. Lett.* 2004, *6*, 185.
- (12) Nau, W. M.; Mohanty, J. *Int. J. Photoenergy* 2005, *7*, 133.
- (13) Koner, L. A.; Nau, W. M. *Supramol. Chem.* 2006, *In press*.
- (14) Mohanty, J.; Nau, W. M. *Angew. Chem.-Int. Edit.* 2005, *44*, 3750.
- (15) Mohanty, J.; Bhasikuttan, A. C.; Nau, W. M.; Pal, H. *J. Phys. Chem. B* 2006, *110*, 5132.
- (16) Lagona, J.; Mukhopadhyay, P.; Chakrabarti, S.; Isaacs, L. *Angew. Chem. Int. Edit.* 2005, *44*, 4844.
- (17) Abrams, C. F.; Delle Site, L.; Kremer, K. *Phys. Rev. E* 2003, *67*.



## Simulation tools

The molecular dynamics simulations reported in this PhD thesis were performed on the clusters of the Theoretical Physical Chemistry group of Prof. Florian Müller-Plathe at the International University Bremen and at the Technische Universität Darmstadt. The cluster in Darmstadt is built of PJ-OPT/HPCF nodes and was supplied by the company TRANSTEC. Additional molecular dynamics calculations were carried out on IBM p575 machines of Hessische Hochleistungsrechner located at Technische Universität Darmstadt. Molecular dynamics as well as quantum calculations were also done on the p690+ IBM machines located in Forschungszentrum Jülich.

For carrying out molecular dynamics simulations, the package YASP was used. The package was developed earlier by Prof. Florian Müller-Plathe and parallelized by myself for shared memory architectures using OpenMP. In order to perform quantum calculations, the Amsterdam Density Functional software package developed and supported by the company SCM was employed.





## Publications

This thesis has led to the following publications:

K.B. Tarmyshov, F. Müller-Plathe. Parallelizing a Molecular Dynamics Algorithm on a Multiprocessor Workstation Using OpenMP. *J. Chem. Inf. Model.* 2005, 45, 1943-1952.

K.B. Tarmyshov, F. Müller-Plathe. Ion Binding to Cucurbit[6]uril: Structure and Dynamics. *J. Phys. Chem. B* 2006, 110(29), 14463-14468.

K.B. Tarmyshov, F. Müller-Plathe. The Interface between Platinum(111) and Liquid Isopropanol: A Model for Molecular Dynamics Studies. *J. Chem. Phys.* submitted.



Konstantin B. Tarmyshow  
Nieder-Ramstädter-Str. 185C  
64285 Darmstadt  
Germany

Darmstadt, den 15. Dezember, 2006

## Eidesstattliche Erklärung

Ich erkläre hiermit an Eides Statt, dass ich meine Dissertation selbständig und nur mit den angegebenen Hilfsmitteln angefertigt habe.

---

(Konstantin B. Tarmyshow)



Konstantin B. Tarmyshov  
Nieder-Ramstädter-Str. 185C  
64285 Darmstadt  
Germany

Darmstadt, den 15. Dezember, 2006

## Erklärung

Ich erkläre hiermit, noch keinen Promotionsversuch unternommen zu haben.

---

(Konstantin B. Tarmyshov)



# Lebenslauf

## Personal data

Name	Konstantin B. Tarmyshov
Date of birth	March 15, 1980
Date of birth	Tyup, Kyrgyz Republic
Citizenship	Russian Federation

## School education

1986 – 1994	Primary and secondary school N7, Kara-Balta, Kyrgyzstan
1994 – 1996	Gymnasium N6, Kara-Balta, Kyrgyzstan
1996 – 1997	Specialized Scientific Study Center of Novosibirsk State University, Novosibirsk, Russia

## Higher education

1997 – 2001	Novosibirsk State University, Novosibirsk, Russia Bachelor of Science degree in Physics
2001 – 2003	Novosibirsk State University, Novosibirsk, Russia Master of Science in Physics
2003 – 2005	International University Bremen, Bremen, Germany Computational Chemistry; PhD student.
2005 – 2006	Technical University Darmstadt, Darmstadt, Germany Computational Chemistry; PhD student.

## Work experience

1999 (approx. 2 months)	Interviewing center, Novosibirsk, Russia Interviewer for different surveys for “FOM: Public Opinion Foundation”, Avtovaz, etc.
2000 – 2001	Unisoft-Plus Software company, Novosibirsk, Russia <u>Position:</u> C++ developer
2001 (04-07)	FTC IT consulting company, Novosibirsk, Russia <u>Position:</u> C++ developer
2001 – 2003	Utilex IT consulting company, Novosibirsk, Russia <u>Position:</u> C++ developer
2001 – 2003	Novosibirsk State University, Novosibirsk, Russia <u>Position:</u> Teaching assistant
2003 – 2005	International University Bremen, Bremen, Germany <u>Position:</u> Teaching assistant